Available online at www.sciencedirect.com
ScienceDirect
Chemosphere 67 (2007) 1477–1484
CHEMOSPHERE
www.elsevier.com/locate/chemosphere

# Thermochemical decomposition of sewage sludge in $CO_2$ and $N_2$ atmosphere

Charothon Jindarom [a], Vissanu Meeyoo [b,*], Thirasak Rirksomboon [a], Pramoch Rangsunvigit [a]

[a] The Petroleum and Petrochemical College, Chulalongkorn University, 245 Soi Chula 12, Phyathai Road, Patumwan, Bangkok 10330, Thailand
[b] Centre for Advanced Materials and Environmental Research, Mahanakorn University of Technology, 51 Cheum-Sampan Road, Nong Chok, Bangkok 10530, Thailand

Received 21 August 2006; received in revised form 12 December 2006; accepted 15 December 2006
Available online 7 February 2007

**Abstract**

In this study, the effect of $CO_2$ on the thermal conversion of sewage sludge was investigated by means of the thermogravimetric analysis and the batch-type thermal process. The results showed that the kinetics of sewage sludge during thermal treatment under both $N_2$ and $CO_2$ atmospheres are quite similar and can be described by a pseudo bi-component separated state model (PBSM). It was, however, noticed that under $CO_2$ atmosphere, the first reaction was significantly accelerated whereas the secondary reaction temperature was shifted to a lower temperature. The apparent activation energies for the first decomposition reaction under both $N_2$ and $CO_2$ atmosphere, corresponding to the main decomposition typically at 305 °C were similarly attained at ca. 72 kJ $mol^{-1}$, while that of the second decomposition reaction was found to decrease from 154 to 104 kJ $mol^{-1}$ under $CO_2$ atmosphere. The typical reaction order of the decomposition under both $N_2$ and $CO_2$ atmosphere was in the range of 1.0–1.5. The solid yield was slightly reduced while the gas and liquid yields were somewhat improved in the presence of $CO_2$. Furthermore, $CO_2$ was found to influence the liquid product by increasing the oxygenated compounds and lessening the aliphatic compounds through the insertion of $CO_2$ to the unsaturated compounds resulting in the carboxylics and the ketones formation.


*Keywords:* Sewage sludge; Thermal decomposition; Kinetics; Mass spectrometry

## 1. Introduction

Since last few years, the amount of sewage sludge generated has increased due to the growth of urban wastewater plants (Kress et al., 2004; Lundin et al., 2004). Pyrolysis, thermal decomposition, is considered as a promising technique to simultaneously treat and stabilize sewage sludge. From pyrolysis, three types of product; gas, liquid and solid, are generated. The process conditions can be optimized to maximize the production of these products depending on a specific application (Meier and Faix, 1999; Inguanzo et al., 2002). The liquid products have a potential to be modified to use as an alternative energy resource and a raw material for chemicals (Yaman, 2004). The solid can be used as an adsorbent (László et al., 1997). The gas product from sewage sludge decomposition is mainly composed of $CO_2$. In a commercial-scaled pyrolysis plant, it has to be operated under relatively oxygen-free atmosphere. Therefore, recycling a gas product stream, to provide such an atmosphere, seems to be an economical way. However, such a reactive atmosphere may significantly influence the yields and quality of the products (Minkova et al., 2000). Most of literatures report only the effect of $CO_2$ on the solid product (Teng et al., 1997; Minkova et al., 2000) but there are few publications focusing on the gas and liquid products. In this study, the thermal decomposition of sewage sludge

* Corresponding author. Tel.: +66 2988 3655x108; fax: +66 2988 4039.
*E-mail address:* vissanu@mut.ac.th (V. Meeyoo).

0045-6535/$ - see front matter © 2007 Elsevier Ltd. All rights reserved.
doi:10.1016/j.chemosphere.2006.12.066

under either $N_2$ or $CO_2$ atmosphere was studied in order to understand the effects of different atmospheric gases used on the kinetics of reaction, product yields and quality of products.

## 2. Experimental

### 2.1. Sewage sludge

Sewage sludge from an urban wastewater treatment plant was selected in this study. The sewage sludge collection method and sample preparation can be found elsewhere (Thipkhunthod et al., 2006). The sludge compositions are mainly volatile matters and ash content, 43% and 46%, respectively. The sludge contains a relatively small amount of moisture and fixed carbon with 6% and 5%, respectively. The empirical formula of the dried sewage sludge, $(C_6H_{11}O_{4.4}N_{0.8}S_{0.2})_n$ which is calculated from the ultimate analysis are compared to the pure cellulose $(C_6H_{10}O_5)_n$.

### 2.2. Thermochemical conversion

#### 2.2.1. Thermogravimetric analysis (TGA)

Thermal decomposition of sewage sludge was carried out using a TG7 Perkin–Elmer thermogravimetric analyzer under either $N_2$ or $CO_2$ atmosphere. Typically, ca. 5 mg of sample were used for each run under non-isothermal conditions. The sample was heated up from ambient temperature to 105 °C and held at this temperature for approximately 10 min to ensure that free-water was completely removed. Then, the sample was further heated to 800 °C with a heating rate between 5 and 20 °C $min^{-1}$. Three repeated experiments were accomplished for data confirmation. The thermogravimetric and differential thermogravimetric (TG–DTG) data were used to differentiate the pyrolysis behavior as well as to provide the estimation of the kinetic parameters.

#### 2.2.2. Batch-type thermal decomposition

The thermal decomposition of the sewage sludge under either $N_2$ or $CO_2$ atmosphere was carried out in a horizontal stainless-steel tubular reactor with an outer diameter of 190.5 mm placed in an electrical furnace. Approximately 5 g of the sample were placed in the reactor between the two layers of quartz wool. The reactor temperature was set at the desired temperatures between 350 and 650 °C. The pyrolysis products were swept out off the reactor and passed through a condenser immersed in a mixture of ice and acetone. The uncondensable gas was collected by a Tedlar® gas sampling bag. At the end of each experiment, the solid residue and condensable liquid were weighed for the evaluation of the product yields. The gas yield was obtained by difference. The products from the pyrolysis were named using *AX* codes, where *A* represents the pyrolysis atmosphere, which is either N for $N_2$ or C for $CO_2$, and *X* represents the pyrolysis temperature.

### 2.3. Product analysis

The uncondensable vapor was chromatographically analyzed using a Shimadzu GC 8A fitted with a thermal conductivity detector. A CTR I (Alltech) packed column was used to separate the gas product under isothermal condition at 50 °C. The injection and a detector temperature was 120 °C.

The condensable liquid was analyzed using a Thermo-Finnigan Trace GC 2000 gas chromatograph coupled with a PolarizQ mass spectrometer. The separation was carried out with a 30 m × 0.25 mm capillary column coated with a 0.25 μm thick film of 5% phenylmethylpolysiloxane. Helium was employed as a carrier gas at a flow of 1.0 ml $min^{-1}$. The initial oven temperature of 40 °C was held for 5 min and then programmed from 40 to 300 °C at 5 °C $min^{-1}$ when isothermally held for 30 min. Splitless injection was carried out at 300 °C and the purge valve was on for 1 min. The ion source and mass transfer line temperatures were 230 and 325 °C, respectively. Data were collected in a full-scan mode with the $m/z$ ratios between 10 and 300, and with a 5-min solvent delay. The identification of compounds was performed by comparing the mass spectrum of the sample with the NIST mass spectra library. The percentage of compounds was calculated from the peak area of the total ion chromatogram (TIC). This method does not give quantitative results but is suitable for comparing the relative proportions of the compounds as used by other authors (Goncalves et al., 1997; Marin et al., 2002; Domínguez et al., 2003).

## 3. Results and discussion

### 3.1. Thermogravimetric analysis (TGA)

Typical TG and DTG curves of sewage sludge decomposition under $N_2$ and $CO_2$ atmospheres are shown in Fig. 1a. The temperatures corresponding to the peaks in the DTG curves are summarized in Table 1. The decomposition of sewage sludge presents incomplete separation of the two decomposition steps. For decomposition under $CO_2$ atmosphere, the first step is between 200 and 370 °C and peak at ca. 305 °C. The second step is between 370 and 600 °C and peak at ca. 425 °C. On the other hand, for decomposition under $N_2$ atmosphere, the first step is between 200 and 420 °C and peak at ca. 305 °C, and the second step is between 420 and 600 and peak at 500 °C. The decomposition of the first and the second steps is accounted to be approximately 60% and 40% of decomposable fraction, respectively. The $T_{90\%}$, the temperature at which 90% of sludge was decomposed, is ca. 540 °C.

The decomposition temperature of the sludge is comparable to those of various materials which can be found elsewhere. The decomposition at 300–350 °C was found to be the decomposition of hemicellulose (Müller-Hagedon et al., 2003), cellulose (Grønli et al., 2002; Müller-Hagedon et al., 2003), micro algae (Peng et al., 2001), leather

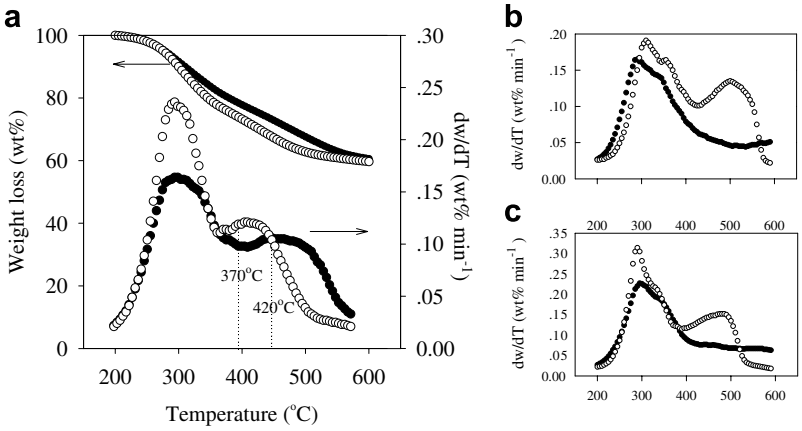


Fig. 1. TG and DTG profiles of the sewage sludge decomposition under (●) $N_2$ and (○) $CO_2$ atmosphere with a heating rate = 20 °C $min^{-1}$: (a) this work (b) type III* and (c) type V* (*source: Thipkhunthod et al., 2006).

Table 1
DTG peak temperature in accordance with the sewage sludge decomposition

| Atmosphere | $T_{m1}$[a] (°C) | $T_{m2}$[a] (°C) | $T_{90\%}$[b] (°C) |
|---|---|---|---|
| $N_2$ | 305 ± 6 | 500 ± 9 | 540 ± 4 |
| $CO_2$ | 305 ± 8 | 425 ± 4 | 510 ± 3 |

Notes:
[a] $T_{m1}$ and $T_{m2}$ are the peak temperatures for the first and second reaction, respectively.
[b] $T_{90\%}$ is the temperature at which 90% of sewage sludge mass was pyrolyzed.

(Heikkinen et al., 2004), and some aliphatic amino acid (Tang et al., 2006), whereas the decomposition at higher temperature, 400–500 °C, is believed to be the decomposition of the complex and/or aromatic structures in various materials such as API separator sludge (Punnaruttanakun et al., 2003), bituminous coal (Folgueras et al., 2005) and some plastics (Chen and Jeyaseelan, 2001).

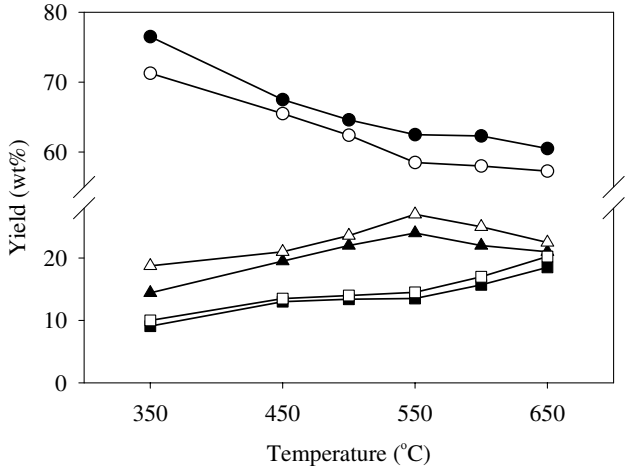


Fig. 2. Variation of yields of solid (●, ○), liquid (▲, △) and gas (■, □) products as a function of temperature. Filled symbol represents the $N_2$ pyrolysis and open symbol represents the $CO_2$ pyrolysis.

By decomposition under $CO_2$ atmosphere, the two steps of the decomposition can still be observed. The magnitude of the DTG curve of the first step increases while that of

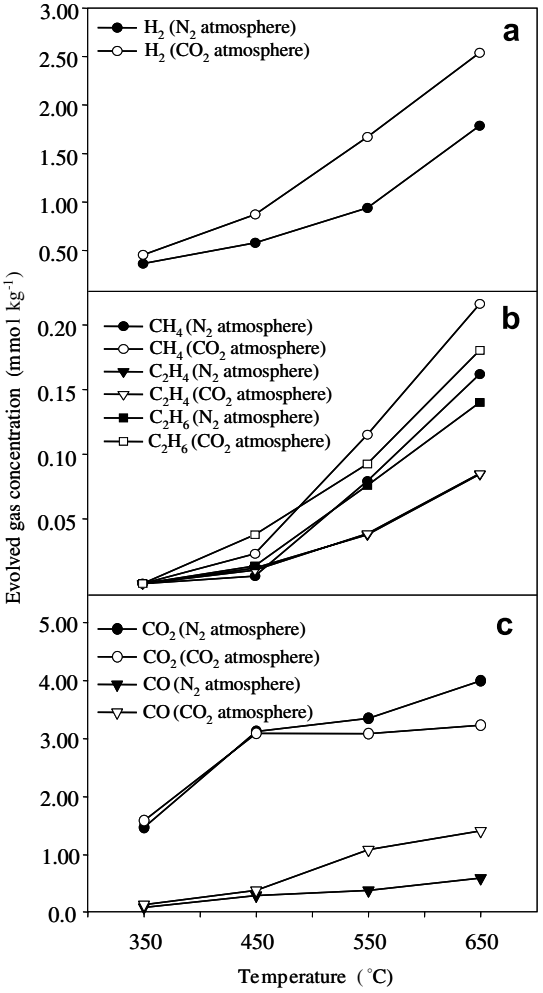


Fig. 3. Evolved gas concentrations obtained from the sewage sludge decomposition under $N_2$ and $CO_2$ atmosphere: (a) $H_2$, (b) $CH_4$, $C_2H_4$ and $C_2H_6$, (c) CO and $CO_2$.

the second step is relatively constant. Moreover, the DTG peak temperature of the second step shifts to a lower temperature, from 500 to 425 °C, and the shape of the peak becomes narrow corresponding to a decrease in $T_{90\%}$. It might be due to the reactivity of $CO_2$ at this temperature range for enhancement of the decomposition by direct heterogeneous oxidation of fixed carbon and volatile matter in the sewage sludge. Therefore, TGA of the two additional sources of the sewage sludge which are defined as types III and V according to the Thipkhunthod et al., 2006, and was studied and their DTG profiles are also shown in Fig. 1b and c. The result confirmed that the reactivity of $CO_2$ on the sewage sludge decomposition was still observed. Moreover, the similar findings were found in the case of the decomposition of some biomass (Encinar et al., 1998), phenol–formaldehyde sphere in the presence of $CO_2$ (Kim et al., 2004), and the decomposition of sewage sludge in the presence of oxygen (Calvo et al., 2004) including the co-combustion of coal and sewage sludge (Folgueras et al., 2005).

### 3.2. Kinetic modeling

With the result of $CO_2$ reactivity, the kinetic parameters were extracted for comparison purpose. As shown in Fig. 1, the decomposition of the sewage sludge as a function of temperature under either $N_2$ or $CO_2$ atmosphere occurs in two steps. Thus, the pseudo bi-component separated state model (PBSM) was reasonably adopted to describe the kinetics of the sewage sludge decomposition. Although the decomposition reactions exhibit incomplete separation, PBSM model can be applied and the obtained kinetic parameters are in good agreement with others method (Müller-Hagedon et al., 2003). With the PBSM, the sludge was considered as two pseudo components and individually decomposed over a temperature range, which can be written as follows:

$$\frac{dx}{dT} = \begin{cases} \dfrac{w_{10} - w_{1\infty}}{w_{10} - w_{2\infty}} \dfrac{dx_1}{dT} & w_{10} < w < w_{1\infty}, \\ \dfrac{w_{20} - w_{2\infty}}{w_{10} - w_{2\infty}} \dfrac{dx_2}{dT} & w_{20} < w < w_{2\infty}, \end{cases}$$

where

$$\frac{dx_1}{dT} = \frac{A_1}{\beta} \exp\left(-\frac{E_1}{RT}\right) f_1(x_1) \qquad w_{10} < w < w_{1\infty},$$

$$\frac{dx_2}{dT} = \frac{A_2}{\beta} \exp\left(-\frac{E_2}{RT}\right) f_2(x_2) \qquad w_{20} < w < w_{2\infty},$$

and $x$ is the mass loss fraction; $\beta$ is the heating rate; $A$ is the frequency factor; $E$ is the activation energy; $R$ is the universal gas constant; $T$ is the absolute temperature and $f(x)$ represents the hypothetical model of the reaction mechanism or 'model function', which can be expressed by $n$th order of reaction, $f(x) = (1 - x)^n$. Subscripts 1 and 2 correspond to the pseudo components 1 and 2, respectively, as well as subscripts 0 and $\infty$ correspond to the initial and final mass

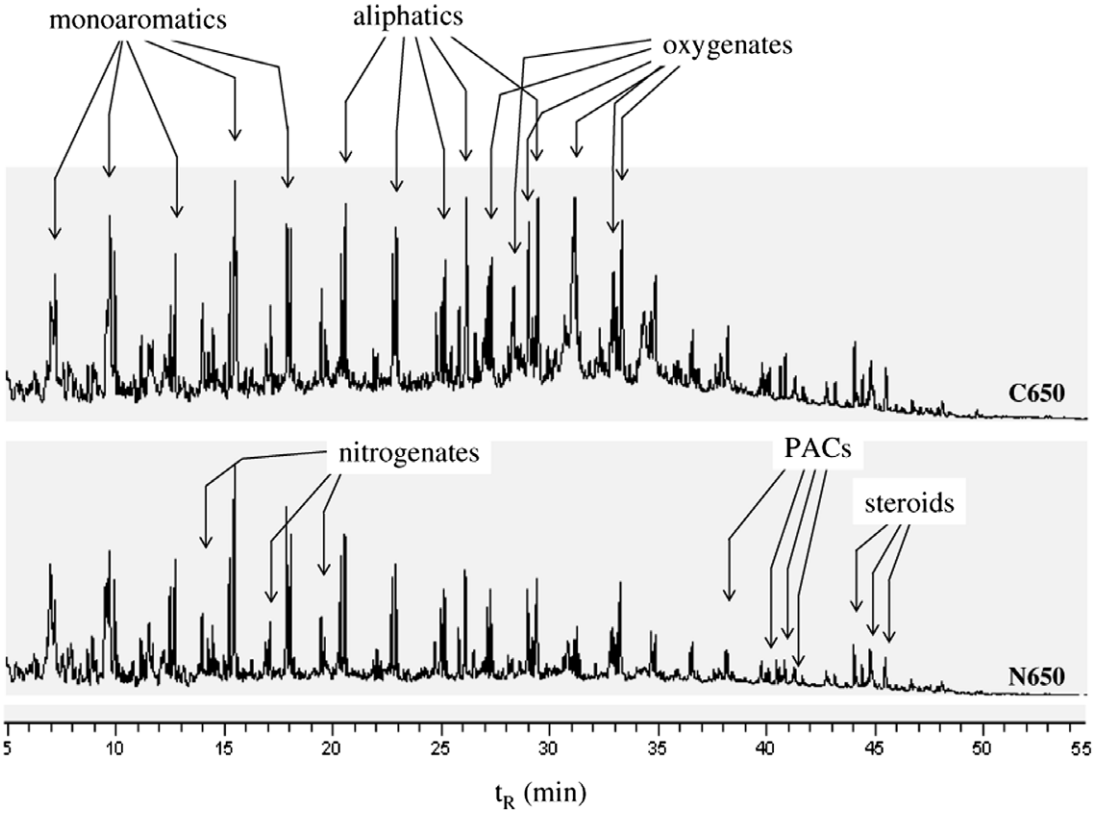


Fig. 4. Typical TIC chromatograms of the liquid product obtained at 650 °C.

Table 2
Relative proportions (% area) of the chemical compounds containing in liquid product obtained from the decomposition of the sewage sludge under $N_2$ and $CO_2$ atmosphere

| Peak | Compound | N350 | N450 | N550 | N650 | C350 | C450 | C550 | C650 |
|---|---|---|---|---|---|---|---|---|---|
| 1 | Benzene | 2.59 | 1.84 | 1.63 | 0.32 | 4.99 | 2.14 | 2.28 | 2.42 |
| 2 | Toluene | 1.65 | 2.22 | 2.35 | 1.26 | 1.00 | 1.89 | 1.83 | 1.69 |
| 3 | Xylene | 0.42 | 1.22 | 2.48 | 4.24 | 0.59 | 5.09 | 4.11 | 3.62 |
| 4 | Styrene | 0.36 | 3.17 | 4.02 | 5.46 | 1.52 | 4.64 | 5.26 | 5.04 |
| 5 | 2,4-Dimethyl-1H-pyrole | 1.83 | 0.57 | 0.82 | 0.58 | | | | |
| 6 | Phenol | 0.60 | 3.10 | 2.94 | 5.97 | 3.65 | 5.44 | 4.51 | 5.14 |
| 7 | Heptane | 2.49 | 0.92 | 1.18 | 2.08 | | 1.73 | 2.84 | 2.21 |
| 9 | 4-Ethyl-2-methyl-pyrrole | | 0.30 | 0.33 | 0.73 | 1.58 | 0.11 | 0.12 | 0.14 |
| 10 | Limonene | | 1.13 | 1.24 | 1.67 | 0.22 | 0.56 | 0.63 | 0.59 |
| 11 | Indene | 0.17 | | | 0.35 | 0.06 | 0.22 | 0.23 | 0.27 |
| 12 | Isopinocarveol | 0.22 | 0.55 | 0.56 | 1.00 | | | | |
| 13 | 1-(1-Cyclohexen-1-yl) ethanone | 1.11 | 0.46 | 0.55 | 2.68 | | | | |
| 14 | 6-Nonynoic acid | 1.28 | | | | 0.35 | 0.64 | 0.71 | 0.63 |
| 15 | 2-Methoxy benzenamine | 0.90 | | | | 1.07 | 1.26 | 1.63 | 1.41 |
| 17 | 4-Methyl phenol | 1.24 | 3.72 | 3.59 | 5.03 | | 4.12 | 2.37 | 2.42 |
| 18 | 3-Carbamic acid methyl ester | | | | | 2.22 | 3.79 | 5.21 | 5.06 |
| 19 | 1-(1-Cyclohexen-1-yl) ethanone | 1.41 | 1.63 | 2.02 | 4.77 | | | | |
| 20 | 5-Methyl-2-hexanone | 0.19 | | | | | | | |
| 21 | Octane | 0.21 | 0.95 | 1.09 | 1.18 | 0.35 | 0.80 | 1.50 | 1.50 |
| 22 | 5H-1-Pyrindine | 0.36 | 0.20 | 0.21 | 0.24 | 0.26 | 0.26 | 0.25 | 0.24 |
| 23 | 1-Azido-2-methyl benzene | 1.48 | 0.12 | 0.00 | 0.10 | 0.52 | 0.35 | 0.62 | 0.34 |
| 24 | Benzenepropanoic acid | | 1.23 | 0.95 | 0.79 | 1.48 | 1.21 | 0.86 | 1.11 |
| 25 | 3-Methyl-1H-indene | 0.77 | | 0.15 | 0.43 | 0.06 | 0.17 | 0.16 | 0.20 |
| 26 | 2-Methyl-5-(1-methylethenyl) cyclohexanol | 1.38 | 0.87 | 0.83 | 0.98 | 0.61 | 0.35 | 0.39 | 0.37 |
| 27 | 2-(Phenylmethyl)-1,3-dioxolane | 0.11 | 0.66 | 0.49 | 0.68 | 0.81 | 0.35 | 0.23 | 0.22 |
| 28 | Iso-Nonane | 0.27 | 0.33 | 0.45 | 0.30 | 0.17 | 0.32 | 0.90 | 0.52 |
| 29 | 2,5-Dimethyl phenol | 0.19 | 0.35 | | 0.66 | 0.16 | 2.88 | 0.65 | 0.84 |
| 30 | 1-Nonene | 0.44 | 0.53 | 0.89 | 1.05 | 0.12 | 0.76 | 1.15 | 0.94 |
| 31 | 2-Methoxy-4-methyl phenol | 0.38 | 0.76 | 0.53 | 0.59 | 0.53 | 0.49 | 0.34 | 0.41 |
| 32 | Nonane | | 1.24 | 1.49 | 2.17 | 0.28 | 0.98 | 1.35 | 1.20 |
| 33 | Pyrridine derivatives | 0.78 | 0.17 | 0.21 | 0.28 | 0.08 | 0.19 | 0.20 | 0.20 |
| 34 | Mono alkylpyridine | 0.15 | 1.71 | 1.41 | 1.73 | 1.65 | 1.48 | 0.00 | 0.00 |
| 35 | 2-Propyl phenol | 0.77 | 0.33 | 0.47 | 0.57 | 0.00 | 0.37 | 0.42 | 0.35 |
| 36 | Butyl butanoate | 1.03 | 0.76 | 0.65 | 0.80 | 1.22 | 0.61 | 0.74 | 0.61 |
| 37 | 1-Decene | 3.23 | 0.87 | 1.54 | 2.39 | 0.55 | 1.07 | 1.21 | 1.31 |
| 38 | Decane | | 5.21 | 4.74 | 5.00 | 7.43 | 5.21 | 5.30 | 6.01 |
| 39 | Indole | | 1.18 | 1.47 | 1.27 | | | | |
| 40 | Thiophene derivatives | 0.35 | | | 0.35 | 0.00 | 0.23 | 2.80 | 2.48 |
| 41 | Butyl phenyl ethers | 0.90 | 0.30 | 0.24 | 0.39 | 0.34 | 0.31 | 0.30 | 0.38 |
| 42 | Pentyl thiophenes | 0.46 | 0.82 | 0.91 | 1.03 | 0.84 | 0.57 | 0.42 | 0.29 |
| 43 | Butyl benzoate | 0.51 | 1.11 | 1.03 | 1.30 | 0.02 | 0.81 | 0.88 | 0.95 |
| 44 | 1-Undecene | 0.42 | 2.24 | 2.44 | 3.44 | 0.00 | 1.98 | 2.42 | 2.31 |
| 45 | Undecane | 0.61 | 0.00 | 1.63 | 2.16 | 0.34 | 1.30 | 1.58 | 1.53 |
| 46 | Iso-Dodecene | 0.36 | 1.32 | 1.21 | 1.19 | 0.00 | 1.23 | 0.13 | 1.06 |
| 47 | Iso-Dodecane | 1.27 | 0.84 | 0.76 | 0.69 | 0.40 | 0.60 | 0.75 | 0.67 |
| 48 | 1-Dodecene | 1.67 | 1.26 | 1.70 | 1.30 | 0.81 | 1.80 | 2.06 | 2.13 |
| 49 | Dodecane | 1.18 | 1.89 | 2.16 | 1.82 | | | | |
| 50 | Naphthalene | 0.95 | 0.51 | 0.64 | 0.17 | 0.54 | 0.33 | 0.60 | 0.57 |
| 51 | Quinolein | 0.78 | 0.57 | 0.62 | 0.53 | 0.74 | 0.37 | 0.30 | 0.38 |
| 52 | 1-Tridecene | 0.76 | 1.55 | 1.99 | | 0.92 | 1.08 | 1.47 | 1.44 |
| 52 | Tridecane | 1.01 | 1.42 | 1.62 | 1.27 | 0.68 | 1.61 | 1.63 | 1.45 |
| 54 | Iso-Tetradecane | 1.20 | 1.34 | 1.33 | 0.43 | 0.82 | 0.81 | 0.80 | 0.89 |
| 55 | 1-Tetradecene | 1.82 | 1.12 | 1.27 | 0.93 | 0.78 | 0.85 | 1.38 | 1.27 |
| 56 | Tetradecane | 0.67 | 1.60 | 0.18 | 1.26 | 0.72 | 1.22 | 1.71 | 1.74 |
| 57 | Acenaphthalene | 4.32 | 1.22 | 0.91 | 0.59 | 0.62 | 0.71 | 0.77 | 0.80 |
| 58 | 2-Methyl-1-tetradecene | 1.95 | 4.06 | 3.32 | 1.48 | 3.42 | 2.54 | 2.81 | 2.91 |
| 59 | 2,5-Pentadecadien-1-ol | | 1.27 | 1.18 | 0.56 | 1.50 | 1.01 | 1.17 | 1.14 |
| 60 | 1-Pentadecene | 1.26 | 1.14 | 1.21 | 0.82 | 1.11 | 0.95 | 1.23 | 1.01 |
| 61 | Pentadecane | 0.63 | 1.25 | 1.26 | 0.89 | 0.90 | 1.08 | 1.18 | 1.17 |
| 62 | 1,9-Hexadecadiene | 4.67 | 3.46 | 3.32 | 1.49 | 4.39 | 2.36 | 2.77 | 2.98 |
| 63 | 1-Hexadecene | 0.71 | 0.59 | 0.65 | 0.51 | 0.79 | 0.43 | 0.78 | 0.59 |
| 64 | Hexadecane | | 0.43 | 0.61 | 0.47 | | 0.53 | 0.82 | 0.54 |

(*continued on next page*)

Table 2 (*continued*)

| Peak | Compound | N350 | N450 | N550 | N650 | C350 | C450 | C550 | C650 |
|---|---|---|---|---|---|---|---|---|---|
| 65 | Hexadecanal | 4.30 | 3.63 | 3.16 | 1.53 | 4.84 | 2.35 | 2.92 | 3.07 |
| 66 | Oleic acid | 20.90 | 5.35 | 2.59 | 0.95 | 19.51 | 13.36 | 8.96 | 5.18 |
| 67 | 1-Heptadecene | | 0.40 | 0.51 | 0.39 | 0.50 | 0.53 | 0.80 | 0.66 |
| 68 | Heptadecane | | 0.62 | 0.70 | 0.57 | 0.70 | 0.44 | 0.56 | 0.56 |
| 69 | Hexadecanoic acid | | 0.54 | 0.52 | 0.30 | 1.41 | 0.88 | 0.91 | 0.95 |
| 70 | Hexadecanoic acid 14-methyl | 1.23 | 1.33 | 1.20 | 0.58 | 0.50 | 0.35 | 0.42 | 0.41 |
| 71 | 1-Octadecene | | 0.47 | 0.46 | 0.39 | 0.28 | 0.46 | 0.70 | 0.62 |
| 72 | Octadecane | | 0.53 | 0.60 | 0.51 | 4.27 | 2.25 | 2.15 | 2.61 |
| 73 | Octadecanoic acid | 6.07 | 2.86 | 2.52 | 1.50 | 3.72 | 0.00 | 0.00 | 0.00 |
| 74 | 9-Octadecenamide | 2.84 | 2.26 | 1.80 | 0.86 | 0.64 | 0.27 | 0.60 | 0.63 |
| 75 | Nonadecane | 0.25 | 0.68 | 0.66 | 0.44 | 0.14 | 0.39 | 0.44 | 0.42 |
| 76 | 1-Eicosene | 0.18 | 0.47 | 0.44 | 0.31 | 0.17 | 0.38 | 0.58 | 0.52 |
| 77 | Eicosane | 0.02 | 0.44 | 0.50 | 0.04 | 0.92 | 0.70 | 0.28 | 0.17 |
| 78 | 9-Octadecen-12-ynoic acid methyl ester | 0.01 | 0.27 | 0.24 | 0.12 | 0.21 | 0.19 | 0.64 | 0.75 |
| 79 | Uncosene | 0.69 | 1.26 | 1.20 | 0.73 | 0.17 | 2.35 | 0.32 | 0.27 |
| 80 | Uncosane | 0.11 | 0.13 | 0.13 | 0.22 | 0.55 | 0.29 | 0.34 | 0.36 |
| 81 | Docosane | 0.34 | 0.58 | 0.67 | 0.40 | 0.36 | 0.31 | 0.36 | 0.31 |
| 82 | 1-Eicosanol | 0.55 | 0.42 | 0.37 | 0.16 | 1.32 | 0.46 | 0.38 | 0.38 |
| 83 | Eicosanoic acid | 0.18 | 0.46 | 0.38 | 0.18 | 1.07 | 0.61 | 0.57 | 0.57 |
| 84 | *N*-methyl-1-octadecanamine | 1.09 | 0.50 | 0.69 | 0.41 | 0.42 | 0.36 | 0.59 | 0.48 |
| 85 | Undecanoic acid | 0.76 | 1.00 | 0.83 | 0.63 | 0.33 | 0.20 | 0.26 | 0.21 |
| 86 | Tricosane | 0.14 | 0.48 | 0.50 | 0.70 | 0.22 | 0.22 | 0.33 | 0.31 |
| 87 | Docosanoic acid | 0.20 | 0.36 | 0.31 | 0.25 | 1.97 | 0.81 | 0.77 | 0.70 |
| 88 | 1-Tetracosene | 0.15 | 0.38 | 0.44 | 0.63 | 1.19 | 0.47 | 0.48 | 0.44 |
| 89 | 3-Cloestene | 0.78 | 1.07 | 1.14 | 1.04 | 0.98 | 0.41 | 0.34 | 0.35 |
| 90 | Cholestene | 0.45 | 0.65 | 0.65 | 0.65 | 0.62 | 0.30 | 0.26 | 0.22 |
| 91 | Cholestene | 0.84 | 1.49 | 1.49 | 1.39 | 1.76 | 0.91 | 0.86 | 0.72 |
| 92 | Cholestene | 0.87 | 1.22 | 1.28 | 1.17 | 0.53 | 0.22 | 0.18 | 0.18 |
| 93 | Cholestadiene | 0.19 | 0.27 | 0.27 | 0.26 | 0.20 | 0.10 | 0.06 | 0.06 |
| 94 | Hexadecanoic acid dodecyl ester | 0.25 | 0.13 | 0.10 | 0.09 | 0.12 | 0.07 | 0.05 | 0.05 |
| 95 | 9-Octadecanoic acid dodecyl ester | 0.06 | 0.08 | 0.06 | 0.07 | 0.07 | 0.07 | 0.06 | 0.06 |

percentages, respectively. The derivation can be found elsewhere (Punnaruttanakun et al., 2003; Thipkhunthod et al., 2006). The order of reaction can be estimated by Coats and Redfern approximation method (Coats and Redfern, 1964).

From the kinetics consideration, it was found that the PBSM model explains reasonably well the weight loss of the sewage sludge regardless of the differences of atmospheric gases used. The apparent activation energies for the first and the second steps of decomposition are 71.5 and 153.7 kJ $mol^{-1}$, respectively. These values of the apparent activation energies obtained are in agreement with those reported elsewhere (Conesa et al., 1997; Chen and Jeyaseelan, 2001; Chao et al., 2002). The reasonable values of the order of the reaction were obtained and were found to be 1.5 and 1 for the first and the second decomposition, respectively.

In the presence of $CO_2$, the apparent activation energy and the reaction order for the first step, $E_1 = 72.9$ kJ $mol^{-1}$ and $n = 1.5$, are quite similar to those of $N_2$ atmosphere. The increase in reaction rate at 300 °C seemed to be influenced by the increasing in frequency factor term in the Arrhenius expression. For the second step, the apparent activation energy was decreased (103.9 kJ $mol^{-1}$) while the order of the reaction was constant at unity. Comparison to the decomposition of sewage sludge under oxygen atmosphere, it was reported that the apparent activation energies are in the between 83 and 310 kJ $mol^{-1}$ and the orders of the reaction is varied from 0.05 to 3.8 (Calvo et al., 2004).

### 3.3. Product yields

Fig. 2 shows the yields of the products. Under $N_2$ atmosphere, the solid fraction decreases while the liquid and gas fractions increase as the temperature increases. The trend of the product yield is the same as for the decomposition under $CO_2$ atmosphere. However, a decrease in solid residue is more significant for the decomposition under $CO_2$ atmosphere than that of $N_2$ atmosphere. Moreover, the gas and liquid fractions increase in the presence of $CO_2$. The increases in gas and liquid fractions indicate that $CO_2$ facilitates their formation reaction. Hence, the solid fraction is also decreased. It was found that the decomposition under either $N_2$ or $CO_2$ produces the highest oil yield at 550 °C at which it seems to be an optimum temperature for oil production.

### 3.4. Gases

The main components of the gas product evolved during the decomposition of sewage sludge are $H_2$, $CH_4$, $C_2H_4$, $C_2H_6$, CO and $CO_2$. The evolution profiles of the gas product are shown in Fig. 3. It was found that the amount of all

gas products increases with increasing the temperature under both $N_2$ and $CO_2$ atmosphere. However, the amount of $H_2$, CO, and $CH_4$ formed was found to be higher for the decomposition under $CO_2$ atmosphere. This might be due to the reactions between $CO_2$ and the products as indicated by the decrease in $CO_2$ with increasing pyrolysis temperature (Fig. 3c). It might be postulated that the possible gas phase reactions involving $CO_2$ are as follows:

$$\text{Boudouard reaction}: \quad C + CO_2 \leftrightarrow 2CO \quad \Delta H_{298} = 173 \text{ kJ mol}^{-1} \tag{1}$$

$$\text{Reversed water gas shift}: \quad H_2 + CO_2 \leftrightarrow H_2O + CO \quad \Delta H_{298} = 41 \text{ kJ mol}^{-1} \tag{2}$$

$$\text{Methane dry reforming}: \quad CH_4 + CO_2 \leftrightarrow H_2 + CO \quad \Delta H_{298} = 247 \text{ kJ mol}^{-1} \tag{3}$$

These reactions were suggested to occur at this temperatures range (Chao et al., 2002; Menéndez et al., 2004) and could be catalyzed by the presence of metals in the sewage sludge. Hence, the large amount of CO formed is anticipated as shown in Fig. 3c. Moreover, the increasing of $CH_4$ might be due to the cracking reaction of the organics containing in sewage sludge pronounced by oxidizing ability of $CO_2$ (Fig. 3b).

### 3.5. Liquids

The liquid mainly consists of aqueous and oil fractions. However, only oil fraction is emphasized in this work. Fig. 4 shows the typical TIC chromatograms of the liquid obtained from sewage sludge decomposition under both $N_2$ and $CO_2$ atmospheres. From the chromatograms, the chemical compositions are tentatively identified and quantified (Table 2) and they can be categorized by their functional groups into six classes: (1) monoaromatics and single ring of heterocyclic compounds such as benzene, benzene alkyl derivatives, toluene, xylene, styrene, phenol and its derivatives and pyrrole; (2) aliphatic compounds such as 1-alkenes, *n*-alkanes and their methyl derivatives; (3) oxygenated compounds such as long chain carboxylic acids, esters, aldehydes and ketones; (4) nitrogenated compounds such as amine and amide; (5) Steroids such as cholestene and cholestadiene; and (6) polycyclic aromatic compounds (PACs) such as 1H-indene, methyl-1H-indene, naphthalene and acetonaphthalene.

It was found that the aliphatic, monoaromatic and oxygenated compounds were the main constituents in the pyrolytic liquid as shown in Fig. 5. The amount of the aliphatic and monoaromatic compounds increases while that of the oxygenated compounds decreases with increasing pyrolysis temperature. It was reported (Amen-Chen et al., 2001) that the monoaromatics resulted from the decomposition of a lignin were formed at high temperatures, and were generated by the cycloaddition reaction of alkenes (Domínguez et al., 2005). Moreover, the decarboxylation reaction coupled with either cracking or aromatization would

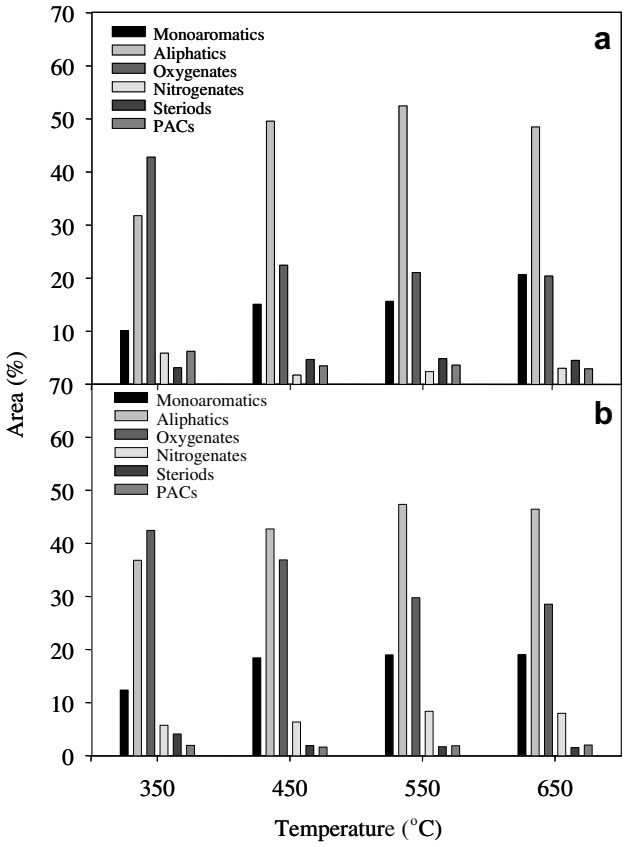


Fig. 5. The distribution of the different chemical classes containing in the liquid product from: (a) $N_2$ atmosphere and (b) $CO_2$ atmosphere.

yield a reduction in the oxygenated compounds but a rise in the aliphatic and the monoaromatic compounds. This is true for pyrolysis under both $N_2$ and $CO_2$ atmospheres but there are somewhat differences in their proportions as shown in Table 2. The distributions of the aliphatic and monoaromatic compounds in the pyrolytic liquid obtained from pyrolysis under $CO_2$ and $N_2$ atmospheres were insignificantly different. However, the amount of oxygenated compounds in the pyrolytic liquid obtained from pyrolysis under $CO_2$ atmosphere was higher than that obtained from pyrolysis under $N_2$ atmosphere. This is believed to be due to the insertion of $CO_2$ into the obtained liquid with the catalysis role of transition metals (Omae, 2006).

Nitrogenates, steroids and PACs, on the other hand, were presented as trace components in the pyrolytic liquid. It should be noted that the liquid product obtained from pyrolysis under $CO_2$ atmosphere contains higher proportion of the nitrogenated compounds but lower proportion of steroids and PACs than the liquid obtained from pyrolysis under $N_2$ atmosphere at the pyrolysis temperatures greater than 450 °C. The increase of nitrogenated compound is mainly due to an increase in proportion of 3-carbamic acid methyl ester (Table 2). This compound appears only in the case of pyrolysis under $CO_2$ atmosphere, therefore, it might be the product resulted from the insertion of $CO_2$ molecules into the nitrogenated compounds.

## 4. Conclusions

It can be concluded that under $CO_2$ atmosphere, two decomposition steps are still observed. The first reaction is significantly accelerated whereas its secondary reaction temperature shifts to a lower temperature. The apparent activation energies for the first reaction of both $N_2$ and $CO_2$ atmospheres, corresponding to the main decomposition typically at 305 °C, are reported at ca. 72 kJ $mol^{-1}$ while that of the second reaction decreases from 154 to 104 kJ $mol^{-1}$ under $CO_2$ atmosphere. The typical reaction order of the decomposition under both $N_2$ and $CO_2$ atmospheres is in the range of 1.0–1.5. The solid yield slightly reduces while the gas and liquid yields are somewhat improved in the presence of $CO_2$. The amount of $H_2$, CO and $CH_4$ formed is high as the sewage sludge is decomposed under $CO_2$ atmosphere. Furthermore, $CO_2$ influences the liquid product by increasing the oxygenated compounds thus decreasing the aliphatic compounds via the insertion of $CO_2$ into the unsaturated aliphatic compounds, resulting in carboxylics and ketones formation.

## Acknowledgements

This work was supported by the Research Unit for Petrochemical and Environmental Catalysts, Ratchadapisek Somphot Endowment Fund, Chulalongkorn University, the Postgraduate Education and Research Programs in Petroleum and Petrochemical Technology (PTT consortium), Chulalongkorn University, and the Thailand Research Fund (under Waste-to-Energy project and Royal Golden Jubilee Ph.D. Program: Grant 0061/45).

## References

Amen-Chen, C., Pakdel, H., Roy, C., 2001. Production of monomeric phenols by thermochemical conversion of biomass: a review. Biores. Technol. 79, 277–299.

Calvo, L.F., Otero, M., Jenkins, B.M., García, A.I., Morán, A., 2004. Heating process characteristics and kinetics of sewage sludge in different atmospheres. Thermochim. Acta 409, 127–135.

Chao, C.G., Chiang, H.L., Chen, C.Y., 2002. Pyrolytic kinetic of sludge from a petrochemical factory wastewater treatment plant – a transition state theory approach. Chemosphere 49, 431–437.

Chen, X., Jeyaseelan, S.J., 2001. Study of sewage sludge pyrolysis mechanism and mathematical modeling. J. Environ. Eng. 126, 585–593.

Coats, A.W., Redfern, J.P., 1964. Kinetic parameters from thermogravimetric data. Nature 201, 68–69.

Conesa, J.A., Marcilla, A., Prats, D., Rodroquez-Pastor, M., 1997. Kinetic study of the pyrolysis of sewage sludge. Waste Manage. Res. 15, 293–305.

Domínguez, A., Menéndez, J.A., Inguanzo, M., Bernard, P.L., Pis, J.J., 2003. Gas chromatographic–mass spectrometric study of the oil fractions produced by microwave-assisted pyrolysis of different sewage sludges. J. Chromatogr. A 1012, 193–206.

Domínguez, A., Menéndez, J.A., Inguanzo, M., Pis, J.J., 2005. Investigations into the characteristics of oils produced from microwave pyrolysis of sewage sludge. Fuel Process. Technol. 86, 1007–1020.

Encinar, J.M., Beltrán, F.J., Ramil, A., González, J.F., 1998. Pyrolysis/gasification of agricultural residues by carbon dioxide in the presence of different additives: influence of variables. Fuel Process. Technol. 55, 219–233.

Folgueras, M.B., Díaz, R.M., Xiberta, J., 2005. Pyrolysis of blends of different types sewage sludge with one bituminous coal. Energy 30, 1079–1091.

Grønli, M.G., Várhegyi, G., Blasi, C.D., 2002. Thermogravimetric analysis and devolatilization kinetics of wood. Ind. Eng. Chem. Res. 41, 4201–4208.

Goncalves, A.R., Schuchardt, U., Meier, D., Faix, O., 1997. Pyrolysis–gas chromatography of the macromolecular fractions of oxidized organocell lignins. J. Anal. Appl. Pyrol., 543–551.

Heikkinen, J.M., Hordijk, J.C., Jong, W.D., Spliethoff, H., 2004. Thermogravimetry as a tool to classify waste components to be used for energy generation. J. Anal. Appl. Pyrol. 71, 883–900.

Inguanzo, M., Domínguez, A., Menéndez, J.A., Blano, C.G., Pis, J.J., 2002. On the pyrolysis of sewage sludge: the influence of pyrolysis conditions on solid, liquid and gas fractions. J. Anal. Appl. Pyrol. 63, 209–222.

Kim, Y.J., Kim, M.I., Yun, C.H., Chang, J.Y., Park, C.R., Inagaki, M., 2004. Comparatives study of carbon dioxide and nitrogen atmospheric effects on the chemical structure changes during pyrolysis of phenol–formaldehydes spheres. J. Colloid Interf. Sci. 274, 555–562.

Kress, N., Herut, B., Galil, B.S., 2004. Sewage sludge impact on sediment quality and benthic assemblages off the Mediterranean coast of Israel – a long-term study. Mar. Environ. Res. 57, 213–233.

László, K., Bóta, A., Nagy, L.G., 1997. Characterization of activated carbons from waste materials by adsorption from aqueous solutions. Carbon 35 (5), 593–598.

Lundin, M., Olofsson, M., Pettersson, G.J., Zetterlund, H., 2004. Environmental and economic assessment of sewage sludge handling options. Resour. Conserv. Recycl. 41, 255–278.

Marin, N., Collura, S., Sharypov, V.I., Beregovtsova, N.G., Baryshnikov, S.V., Kutnetzov, B.N., Cebolla, V., Weber, J.V., 2002. Copyrolysis of wood biomass and synthetic polymer mixtures. Part II: characterization of the liquid phases. J. Anal. Appl. Pyrol. 65, 41–55.

Meier, D., Faix, O., 1999. State of the art of applied fast pyrolysis of lignicellulosic materials – a review. Biores. Technol. 68, 71–77.

Menéndez, J.A., Domínguez, A., Inguanzo, M., Pis, J.J., 2004. Microwave pyrolysis of sewage sludge: analysis of the gas fraction. J. Anal. Appl. Pyrol. 71, 657–667.

Minkova, V., Marinov, S.P., Zanzi, R., Bjornbom, E., Budinova, T., Stefanova, M., Lakov, L., 2000. Thermochemical treatment of biomass in a flow of steam or in a mixture and carbon dioxide. Fuel Process. Technol. 62, 45–52.

Müller-Hagedon, M., Bockhorn, H., Krebs, L., Müller, U., 2003. A comparative kinetic study on the pyrolysis of three different wood species. J. Anal. Appl. Pyrol. 68–69, 231–249.

Omae, I., 2006. Aspect of carbon dioxide utilization. Catal. Today 115, 33–52.

Peng, W., Wu, Q., Tu, P., Zhao, N., 2001. Pyrolytic characteristics of microalgae as renewable energy source determined by thermogravimetric analysis. Biores. Technol. 80, 1–7.

Punnaruttanakun, P., Meeyoo, V., Kalambaheti, C., Rangsunvigit, P., Rirksomboon, T., Kitiyanan, B., 2003. Pyrolysis of API separator sludge. J. Anal. Appl. Pyrol., 547–560.

Teng, H., Ho, J.A., Hsu, Y.F., 1997. Preparation of activated carbons from bituminous coals with $CO_2$ activation influence of coal oxidation. Carbon 35, 275–283.

Thipkhunthod, P., Meeyoo, V., Rangsunvigit, P., Kitiyanan, B., Siemanond, K., Rirksomboon, T., 2006. Pyrolytic characteristics of sewage sludge. Chemosphere 64, 955–962.

Tang, W., Wang, C., Chen, D., 2006. An investigation of the pyrolysis kinetics of some aliphatic amino acids. J. Anal. Appl. Pyrol. 75, 49–53.

Yaman, S., 2004. Pyrolysis of biomass to produce fuels and chemical feedstocks. Energ. Convers. Manage. 45, 651–671.